Journal of the European Ceramic Society 22 (2002) 777–783

www.elsevier.com/locate/jeurceramsoc

The effect of rare-earth oxide addition on the hot-pressing of magnesium silicon nitride

Shukiko Tanaka[a], Kiyoshi Itatani[a,*], Hiroshi Uchida[a], Mamoru Aizawa[a], Ian J. Davies[b], Hiroshi Suemasu[c], Akira Nozue[c], Isao Okada[a]

[a]*Department of Chemistry, Faculty of Science and Engineering, Sophia University, 7-1, Kioi-cho, Chiyoda-ku, Tokyo 102-8554, Japan*

[b]*Advanced Fibro-Science, Kyoto Institute of Technology, Matsugasaki, Sakyo-ku, Kyoto 606-8585, Japan*

[c]*Department of Mechanical Engineering, Faculty of Science and Engineering, Sophia University 7-1, Kioi-cho, Chiyoda-ku, Tokyo 102-8554, Japan*

Received 25 January 2001; received in revised form 28 May 2001; accepted 3 June 2001

Abstract

The effect of rare-earth oxide addition (1–5 mass% of Ln_2O_3 addition; Ln = Y, La, Nd, Sm, Gd, Dy, Er, and Yb) on the properties of hot-pressed (1550 °C, 90 min, 31 MPa) magnesium silicon nitride ($MgSiN_2$) compact (ceramic) has been investigated. The role of rare-earth oxide addition on the relative density was classified as follows: (i) positive effect (Y_2O_3, La_2O_3, and Yb_2O_3 addition), (ii) no appreciable effect (Nd_2O_3 and Er_2O_3 addition), and (iii) negative effect (Sm_2O_3, Gd_2O_3, and Dy_2O_3 addition). The grain sizes of the $MgSiN_2$ ceramics with rare-earth oxide addition were almost comparable to or slightly smaller than those of the pure $MgSiN_2$ ceramic. The average Vickers hardness of the $MgSiN_2$ ceramic with 1 mass% of Y_2O_3 addition showed the highest value (21.5 GPa) amongst the $MgSiN_2$ ceramics with rare-earth oxide addition. The thermal conductivity of the $MgSiN_2$ ceramic had a maximum for the case of 1 mass% of Yb_2O_3 addition (26.6 $W{\cdot}m^{-1}{\cdot}K^{-1}$) and was believed to be the highest value so far reported for $MgSiN_2$ ceramic. It was concluded that the relative density and Vickers hardness were best enhanced through the use of Y_2O_3 addition, whereas the addition of Yb_2O_3 was most suitable for enhancing the thermal conductivity.

Keywords: Hot pressing; Mechanical properties; $MgSiN_2$; Rare-earth oxide addition; Thermal properties

1. Introduction

The continuing trend towards miniaturization of electronic integrated circuits and fuel-efficient engine components requires the development of novel materials with high thermal conductivity. It has been suggested that electronically insulating materials with high thermal conductivity, κ, need to possess the following characteristics: (i) simple crystal structure, (ii) low atomic mass, (iii) strong covalent bonding, (iv) low anharmonicity, and (v) high purity.[1] One material that fulfils these requirements is aluminum nitride (AlN) but it has the disadvantages of severe processing conditions and of κ being strongly dependent on the degree of oxygen contamination.[1]

Recently, several researchers[1–7] have focused on magnesium silicon nitride ($MgSiN_2$) as being a potential ceramic with high thermal conductivity, due to $MgSiN_2$ being deducted from AlN by systematic substitution of two Al atoms in the AlN crystal structure by Mg and Si atoms. Furthermore, single-phase $MgSiN_2$ may easily be prepared using conventional techniques.[4,5] The reported maximum thermal conductivity of $MgSiN_2$ so far obtained has been 25 $W{\cdot}m^{-1}{\cdot}K^{-1}$ [1,3] and significantly lower compared to the theoretical value of 320 $W{\cdot}m^{-1}{\cdot}K^{-1}$ for AlN.[8] In spite of this, however, $MgSiN_2$ ceramics may still be an attractive proposition due to their high Vickers hardness (~20 GPa) and low coefficient of thermal expansion (3.8×10^{-6} K^{-1} at 300 K),[9] close to that (3.0×10^{-6} K^{-1}) of silicon (Si). In order to enhance the thermal conductivity of $MgSiN_2$, the following conditions need to be met: (i) full densification upon sintering, (ii) increased grain size, (iii) localization of the secondary oxide phases at the grain triple points, and (iv) reduced number of defects in the grains/lattice; all of which inhibit phonon scattering.

Referring to the first condition, i.e., full densification of $MgSiN_2$ ceramics, Hintzen et al.[3] and the present

* Corresponding author. Tel.: +81-3-3238-3373; fax: +81-3-3238-3361.

E-mail address: itatani@hoffman.cc.sophia.ac.jp (K. Itatani).

0955-2219/02/$ - see front matter
PII: S0955-2219(01)00380-6

authors[6,7] have noted yttrium oxide (Y_2O_3) to be a useful sintering aid in the densification of $MgSiN_2$. Although it might be reasonable to assume that other rare-earth oxides also lead to improved densification and mechanical/thermal properties, no systematic research on this phenomenon has so far been conduced. In view of this, the aim of the present paper is to determine the effect of different rare-earth oxide additions on the densification and mechanical/thermal properties of $MgSiN_2$ ceramics.

2. Experimental procedure

2.1. Starting materials, compaction, and firing

The starting $MgSiN_2$ powder utilized in the present study was prepared by the nitridation of magnesium silicide (Mg_2Si) powder at 1350 °C for 10 min in a nitrogen atmosphere. Yttrium oxide (Y_2O_3), lanthanum oxide (La_2O_3), neodymium oxide (Nd_2O_3), samarium oxide (Sm_2O_3), gadolinium oxide (Gd_2O_3), dysprosium oxide (Dy_2O_3), erbium oxide (Er_2O_3), and ytterbium oxide (Yb_2O_3) (all 99.99% purity, Wako Pure Chemical Ltd., Tokyo) were selected as sintering aids. The rare-earth oxide powders were individually mixed with $MgSiN_2$ powder in quantities ranging from 1–5 mass% using a zirconium oxide (ZrO_2) mortar and pestle in the presence of hexane. After drying, approximately 1.5 g of the mixed powder was uniaxially pressed at 30 MPa to result in a compact with a diameter of 20 mm and thickness of ~2 mm. Each of the compacts was placed in a graphite die and hot-pressed at 1550 °C for 90 min in a nitrogen atmosphere under a pressure of 31 MPa as these conditions had proved most suitable in previous work.[7] The heating rate was 30 °C·min^{-1} up to 1100 °C and 10 °C·min^{-1} up to 1550 °C with the compact being furnace-cooled following the hot pressing procedure.

2.2. Measurements and observation

The relative density of the hot-pressed compact (ceramic) was calculated using the bulk and true densities; the bulk density was determined by measuring the dimensions and mass of the ceramics whereas the true density was determined picnometrically at 25.0 °C following pulverization of the ceramic. Crystalline phases present in the ceramic were characterized using an X-ray diffractometer (XRD) (Model RINT2000, Rigaku Corp., Tokyo) and monochromatic CuK_α radiation at 40 kV and 40 mA, and referenced using Joint Committee on Powder Diffraction Standards (JCPDS) cards. The lattice parameters of the $MgSiN_2$ (orthorhombic system) were determined using 13 XRD reflections (110, 011, 120, 200, 002, 121, 201, 122, 202, 040, 320, 123, and 203) with silicon being used as an internal standard in order to correct the reflection angles.

The microstructure of the ceramic was investigated using a field-emission scanning electron microscope (FE–SEM) (Model S-4500, Hitachi, Tokyo; accelerating voltage, 5.0 kV) after coating the surfaces with Pt–Pd in order to reduce charging effects. Prior to observation by FE-SEM, the grain boundaries were etched using Murakami's reagent.[10] The Vickers hardness, H_v, of the ceramic was measured using an indentation load and time of 9.81 N and 15 s, respectively (Model MVK-E, Akashi Corp., Tokyo). At least ten different regions were evaluated for each ceramic in order to obtain an average value. The fracture toughness, K_{IC}, of the ceramic was calculated on the basis of the following equation:[11]

$$\frac{K_{IC}}{H_v a^{1/2}} = k\left(\frac{c}{a}\right)^{-3/2} \tag{1}$$

where a is the indent radius (mm), c is the radial crack length (mm), and k is an experimental constant (= 0.203). Thermal diffusivity and specific heat data for the ceramic were obtained at 20 °C using a laser-flash technique (Model TC-7000, Shinku-Riko, Tokyo). The thermal conductivity, κ, of a material may be expressed as follows:[12]

$$\kappa = \alpha\rho C_v \tag{2}$$

where α is the thermal diffusivity, ρ is the density, and C_v is the specific heat at constant volume. The specific heats of $MgSiN_2$ ceramics with rare-earth oxide addition were measured using the laser-flash technique.[13]

3. Results and discussion

3.1. Densities and microstructures of $MgSiN_2$ ceramics with rare-earth oxide addition

As reported in previous work,[6,7] the densification of $MgSiN_2$ compacts was promoted by the addition of Y_2O_3 as a sintering aid. In this section, the effect of different rare-earth oxide addition on the density/microstructure of $MgSiN_2$ ceramic was systematically examined. The true (picnometric) and bulk densities of the pure $MgSiN_2$ ceramic were 3.128 and 2.878 g·cm^{-3}, respectively. The true density of the $MgSiN_2$ ceramic was slightly enhanced with increasing amount of rare-earth oxide addition whereas the bulk densities of $MgSiN_2$ ceramics varied according to the kind of rare-earth oxide used as a sintering aid. On the basis of these density data, the relative densities of $MgSiN_2$ ceramics with rare-earth oxide addition were calculated by dividing the bulk densities by the true densities.

Fig. 1 illustrates the trends in relative density for the $MgSiN_2$ ceramics with increasing amounts of rare-earth

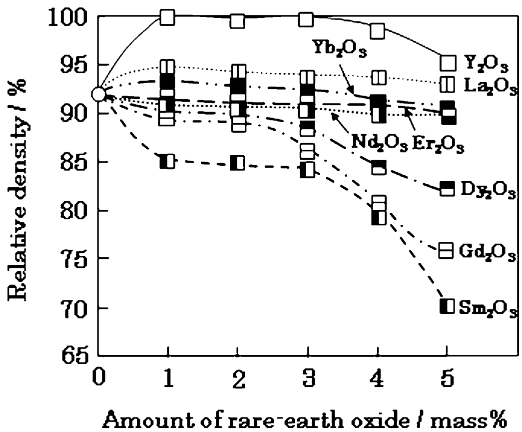

Fig. 1. Effect of rare-earth oxide addition on the relative density of $MgSiN_2$ compact hot-pressed at 1550 °C for 90 min under a pressure of 31 MPa. ○: No addition; □: Y_2O_3 addition; ◫: La_2O_3 addition; ◨: Nd_2O_3 addition; ◧: Sm_2O_3.addition; ⊟: Gd_2O_3 addition; ⬒: Dy_2O_3 addition; ⬓: Er_2O_3 addition; ■: Yb_2O_3 addition.

oxide addition. It should be noted that the relative density of the pure $MgSiN_2$ ceramic was 92.0%. The effect of rare-earth oxide addition on the density of $MgSiN_2$ ceramic could be classified into three main groups, i.e. (i) positive effect (Y_2O_3, La_2O_3, and Yb_2O_3 addition), (ii) no appreciable effect (Nd_2O_3 and Er_2O_3 addition), and (iii) negative effect (Sm_2O_3, Gd_2O_3, and Dy_2O_3 addition). As a comparison, the relative density of the $MgSiN_2$ ceramic with 1 mass% of Y_2O_3 addition attained 99.9%, whereas that of the $MgSiN_2$ ceramic with 5 mass% of Sm_2O_3 addition was only 69.8%. Although no appreciable negative effects were observed below 2 mass% of Dy_2O_3 and Gd_2O_3 addition, further increases above this amount resulted in $MgSiN_2$ ceramics with reduced relative densities.

Microstructures of the $MgSiN_2$ ceramics with rare-earth oxide addition were examined using FE-SEM. Typical FE-SEM micrographs for the polished surfaces and their chemically-etched surfaces of $MgSiN_2$ ceramics with and without rare-earth oxide addition have been presented in Fig. 2. The observation of polished surfaces showed that the number of pores in the $MgSiN_2$ ceramic with Sm_2O_3 addition [Fig. 2(f)] was larger than the numbers of pores in other cases [Fig. 2(a)–(e)]. Referring to the observation of chemically-etched surfaces, the pure $MgSiN_2$ ceramic was composed of polyhedral grains with a typical size of ~1 μm [Fig. 2(a)]. Typical grain sizes of the $MgSiN_2$ ceramics with Y_2O_3 and Yb_2O_3 addition were as low as ~0.5 μm [Fig. 2(b) and (d)]. On the other hand, the $MgSiN_2$ ceramic with 1 mass% of La_2O_3 addition contained grains with a typical size of ~1 μm [Fig. 2(c)]. The grain sizes of the $MgSiN_2$ ceramic with Er_2O_3 and Sm_2O_3 addition ranged from 0.5 to 1 μm [Fig. 2(e) and (f)].

Grain sizes of the $MgSiN_2$ ceramics with rare-earth oxide addition are nearly comparable to, or slightly smaller than those of the pure $MgSiN_2$ ceramic. Such changes in grain sizes of $MgSiN_2$ ceramics by the rare-earth oxide addition were also confirmed by the observation of fracture surfaces, although the SEM micrographs for these fracture surfaces are omitted in this paper.

In order to examine the reactions between $MgSiN_2$ and rare-earth oxides, the crystalline phases were checked using XRD. Typical XRD patterns for the $MgSiN_2$ ceramics with 5 mass% of rare-earth oxide addition have been shown in Fig. 3. The ceramic with Yb_2O_3 addition included $MgSiN_2$,[14] $Yb_2Si_3O_3N_4$,[15] and $Yb_2Si_3O_5N_2$.[16] The ceramics with Sm_2O_3 and Er_2O_3 addition contained $Sm_2Si_3O_3N_4$[17] and $Er_2Si_3O_3N_4$,[18] respectively, as reaction products. Reflection intensities for $Sm_2Si_3O_3N_4$ were much higher compared to those for $Yb_2Si_3O_3N_4$ and $Er_2Si_3O_3N_4$. Although other XRD patterns have not been presented in this work, $Ln_2Si_3O_3N_4$ (Ln = Y, La, Nd, Gd, and Dy) was also detected for each $MgSiN_2$ ceramic with rare-earth oxide addition.

As a typical case, the reaction between $MgSiN_2$ and Yb_2O_3 may be expressed as follows:

$$3MgSiN_2 + Yb_2O_3 \rightarrow Yb_2Si_3O_3N_4 + Mg_3N_2 \quad (3)$$

$$3MgSiN_2 + 2Yb_2O_3 \rightarrow Yb_2Si_3O_5N_2 + 2YbN + Mg_3N_2 + 1/2O_2 \quad (4)$$

Although Mg_3N_2 and YbN were not detected by XRD, it may be the case that they are present as amorphous phases or else evaporated during hot pressing. Densification of the $MgSiN_2$ compact is, therefore, affected by the chemical and thermal stabilities of the reaction products, in particular $Ln_2Si_3O_3N_4$. Comparing the X-ray reflection intensities for $Sm_2Si_3O_3N_4$, $Er_2Si_3O_3N_4$, and $Yb_2Si_3O_3N_4$, the X-ray reflection intensity for $Sm_2Si_3O_3N_4$ was much higher compared to those of $Yb_2Si_3O_3N_4$ and $Er_2Si_3O_3N_4$. This fact suggests that $Sm_2Si_3O_3N_4$ is more chemically and thermally stable compared to either $Yb_2Si_3O_3N_4$ or $Er_2Si_3O_3N_4$. The delay in densification of the $MgSiN_2$ compact by the addition of Sm_2O_3 may, therefore, be attributed to an increase in the amount of $Sm_2Si_3O_3N_4$ formed during hot pressing.

Generally speaking, $Ln_2Si_3O_3N_4$ is a thermally stable compound and possesses a high melting point, e.g. ~1900 °C for $Y_2Si_3O_3N_4$[19] and ~1700 °C for $Sm_2Si_3O_3N_4$.[20] Thus, densification of the $MgSiN_2$ compact with rare-earth oxide addition appears to occur along with the formation of liquid phases and $Ln_2Si_3O_3N_4$. Referring to

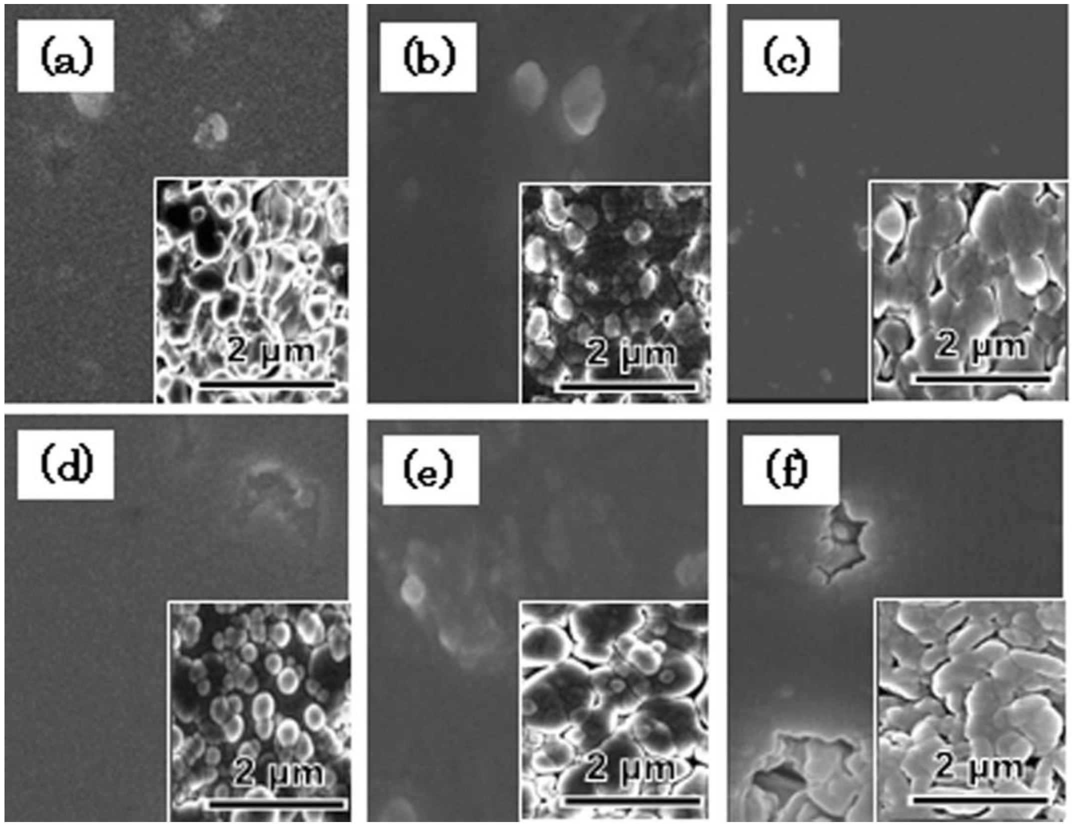

Fig. 2. Typical FE–SEM micrographs for the polished surfaces and their chemically-etched surfaces of $MgSiN_2$ compacts with 1 mass% of rare-earth oxide addition hot-pressed at 1550 °C for 90 min under a pressure of 31 MPa. (a) No addition [relative density (RD): 92.0%]; (b) Y_2O_3 addition (RD = 99.9%); (c) La_2O_3 addition (RD = 94.8%); (d) Yb_2O_3 addition (RD = 93.1%); (e) Er_2O_3 addition (RD = 91.4%); (f) Sm_2O_3 addition (RD = 85.0%).

the liquid composition, Inomata et al.[21] pointed out that a eutectic liquid in the Si_3N_4–$MgSiN_2$ system forms at ~1520 °C. Moreover, as the case of the $MgSiN_2$ ceramic with Y_2O_3 addition indicates, liquid phases in the Si_3N_4–SiO_2–Y_2O_3–YN system may be present at 1550 °C.[22] The liquid composition present during hot pressing is therefore complex and the liquid volume varies according to the type of rare-earth oxide. In addition to this, the amount of liquid phase may be small when the rare-earth oxide is consumed by the formation of $Ln_2Si_3O_3N_4$.[20] The reason why densification of the $MgSiN_2$ compact was retarded by the addition of Sm_2O_3 is explained by the amount of liquid phase present being insufficient for the rearrangement of grains as a result of the solid-state reaction between $MgSiN_2$ and Sm_2O_3 to form $Sm_2Si_3O_3N_4$.

3.2. Mechanical and thermal properties of $MgSiN_2$ ceramics with rare-earth oxide addition

The mechanical and thermal properties of $MgSiN_2$ ceramics with rare-earth oxide addition will be described in this section. The Vickers hardness values for the $MgSiN_2$ ceramics with and without rare-earth oxide

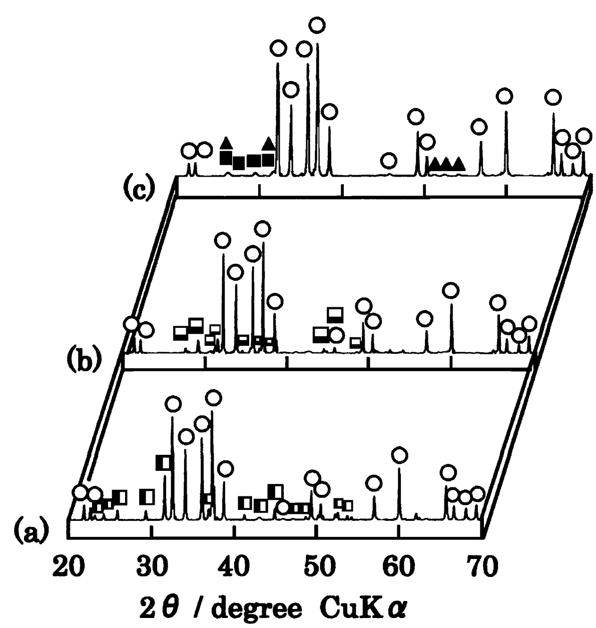

Fig. 3. Typical XRD patterns for the $MgSiN_2$ compacts with 5 mass% of (a) Sm_2O_3, (b) Er_2O_3 and (c) Yb_2O_3 additions hot-pressed at 1550 °C for 90 min under a pressure of 31 MPa. ○: $MgSiN_2$; ◧: $Sm_2Si_3O_3N_4$; ⬓: $Er_2Si_3O_3N_4$; ■: $Yb_2Si_3O_3N_4$; ▲: $Yb_2Si_3O_5N_2$.

addition have been presented in Fig. 4. The Vickers hardness values for the $MgSiN_2$ ceramics with 1 mass% of rare-earth oxide addition were higher compared to those $\geqslant$2 mass% of rare-earth oxide addition. The average Vickers hardness value (21.5 GPa) for the $MgSiN_2$ ceramic with 1 mass% of Y_2O_3 addition was slightly higher than that for the pure $MgSiN_2$ ceramic (20.7 GPa). Average Vickers hardness values for the $MgSiN_2$ ceramics with other rare-earth oxide additions were in the range of 18.1 to 20.6 GPa; nearly comparable to, or slightly lower than, the pure $MgSiN_2$ ceramic value.

The above trends may be correlated to the relative density, grain size, and mechanical properties of the reaction products ($Ln_2Si_3O_3N_4$ and $Ln_2Si_3O_5N_2$) and amorphous materials. The Vickers hardness being enhanced by the addition of Y_2O_3 (21.5 GPa) is attributed chiefly to the high relative density (99.9%) and comparatively small grain size [see Fig. 2(b)]. The general decrease in Vickers hardness with an increasing amount of rare-earth oxide addition ($\geqslant$ 2 mass%) is attributed to an increase in the amount of reaction products.

On the basis of the Vickers hardness data, the effect of rare-earth oxide addition on the fracture toughness and thermal conductivity of the $MgSiN_2$ ceramic was examined. The amount of rare-earth oxide addition was fixed to be 1 mass%, because (i) their relative density and Vickers hardness values being generally higher compared to those ceramics with $\geqslant$2 mass% of rare-earth oxide addition, and (ii) the amount of rear-earth oxide addition should be minimized in order to optimize the mechanical and thermal properties. Note that 1 mass% of Y_2O_3 (the lightest molecular weight (=225.8) among the rare-earth oxides under investigation) corresponds to 0.36 mol% whereas that of Yb_2O_3 [the largest molecular weight (=394.1)] corresponds to 0.21 mol%.

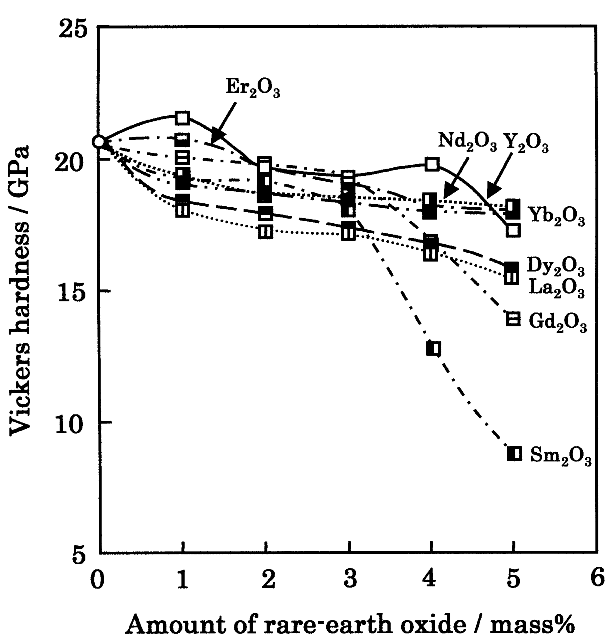

Fig. 4. Effect of rare-earth oxide addition on the average Vickers hardness of $MgSiN_2$ compact hot-pressed at 1550 °C for 90 min under a pressure of 31 MPa. ○: No addition; □: Y_2O_3 addition; ◫: La_2O_3 addition; ◨: Nd_2O_3 addition; ◧: Sm_2O_3 addition; ⊟: Gd_2O_3 addition; ⬒: Dy_2O_3 addition; ⬓:Er_2O_3 addition; ■: Yb_2O_3 addition.

Average values for the fracture toughness and thermal conductivities of $MgSiN_2$ ceramics with 1 mass% of rare-earth oxide addition are listed in Table 1, together with their relative densities and Vickers hardness values. The fracture toughness value of the pure $MgSiN_2$ ceramic was 0.98 $MPa{\cdot}m^{1/2}$, whereas the fracture toughness values of $MgSiN_2$ ceramics with rare-earth oxide addition were around 1 $MPa{\cdot}m^{1/2}$. No appreciable difference in fracture toughness was noted for the $MgSiN_2$ ceramics with rare-earth oxide addition.

Although the thermal conductivity of the $MgSiN_2$ ceramic with 1 mass% of Yb_2O_3 addition reached 26.6 $W{\cdot}m^{-1}{\cdot}K^{-1}$, values for the remaining $MgSiN_2$ ceramics with and without rare-earth oxide addition were in the range of 19.0–21.2 $W{\cdot}m^{-1}{\cdot}K^{-1}$. It should be noted that the thermal conductivity of the $MgSiN_2$ ceramic with 1 mass% of Yb_2O_3 addition (26.6 $W{\cdot}m^{-1}{\cdot}K^{-1}$) is believed to be the highest value so far reported for $MgSiN_2$. In contrast this, the $MgSiN_2$ ceramic with Y_2O_3 addition indicates $\kappa=21.1$ $W{\cdot}m^{-1}{\cdot}K^{-1}$ despite this ceramic possessing the highest relative density (99.9%). It is suggested that the superior thermal conductivity of the $MgSiN_2$ ceramic with Yb_2O_3 addition indicates that phonon scattering may chiefly be retarded through the elimination of some oxygen during hot pressing [see Eqn. (3)], although it should be noted that reaction products, i.e., $Yb_2Si_3O_3N_4$ and $Yb_2Si_3O_5N_2$, were still detected within the $MgSiN_2$ ceramic.

In order to determine the level of oxygen and rare-earth metal ion solid solution into $MgSiN_2$, the lattice parameters of $MgSiN_2$ (orthorhombic system) with rare-earth oxide addition were measured quantitatively using XRD. Although the data have not been presented

Table 1
Average values for the Vickers hardness, fracture toughness, and thermal conductivities of $MgSiN_2$ compacts with 1 mass% of rare-earth oxide addition hot-pressed at 1550 °C for 90 min under a pressure of 31 MPa

Additive	Relative density	Vickers hardness	Fracture toughness	Thermal conductivity
	(%)	(GPa)	($MPa.m^{1/2}$)	($W{\cdot}m^{-1}{\cdot}K^{-1}$)
None	92.0	20.7	0.98	19.8
Y_2O_3	99.9	21.5	1.00	21.1
La_2O_3	94.8	18.1	1.03	22.1
Nd_2O_3	90.0	19.4	1.00	22.3
Sm_2O_3	85.0	19.2	0.97	21.1
Gd_2O_3	89.5	20.0	1.09	21.4
Dy_2O_3	90.9	18.4	1.02	19.0
Er_2O_3	91.4	20.7	0.89	20.4
Yb_2O_3	93.3	19.0	1.01	26.6

in this work, no appreciable change in lattice parameters (compared to that of pure $MgSiN_2$; $a = 0.5272$ nm, $b = 0.6479$ nm, and $c = 0.4987$ nm) was observed due to the addition of rare-earth oxides. It would therefore appear that no significant solid solution exists for either oxygen or rare-earth metal ions into $MgSiN_2$. This assumption is partly supported by Bruls,[23] who reported the solubility limit of oxygen into $MgSiN_2$ to be less than 0.5 mass% in addition to the presence of oxygen-containing reaction products as separate grains in the matrix.

4. Conclusions

The effect of rare-earth oxide addition (1–5 mass%) on the properties of hot pressed (1550 °C, 90 min, 31 MPa) magnesium silicon nitride ($MgSiN_2$) compact (ceramic) has been examined; the rare-earth oxides employed in this work were Ln_2O_3 (Ln = Y, La, Nd, Sm, Gd, Dy, Er, and Yb). The results obtained have been summarized as follows:

1. The relative density of the pure $MgSiN_2$ ceramic was 92.0%. The effects of rare-earth oxide addition on the relative density of $MgSiN_2$ ceramics were classified as follows: (i) positive effect (Y_2O_3, La_2O_3, and Yb_2O_3 addition), (ii) no appreciable effect (Nd_2O_3 and Er_2O_3 addition), and (iii) negative effect (Sm_2O_3, Gd_2O_3, and Dy_2O_3 addition). The $MgSiN_2$ ceramics with 1 mass% of rare-earth oxide addition generally exhibited a higher relative density compared to that of $\geqslant$ 2 mass% of rare-earth oxide addition. The grain sizes of the $MgSiN_2$ ceramics with rare-earth oxide addition were nearly comparable to or slightly smaller than the case of the pure $MgSiN_2$ ceramic.
2. The Vickers hardness value was highest for the $MgSiN_2$ ceramic with 1 mass% of Y_2O_3 addition (21.5 GPa). Fracture toughness values for the $MgSiN_2$ ceramics with and without rare-earth oxide addition were $\sim$1 $MPa{\cdot}m^{1/2}$. The thermal conductivity had a maximum for the $MgSiN_2$ ceramic with 1 mass% of Yb_2O_3 addition (26.6 $W{\cdot}m^{-1}{\cdot}K^{-1}$). It was concluded that the addition of Y_2O_3 into the $MgSiN_2$ compact was most suitable for enhancing the relative density and Vickers hardness whereas the addition of Yb_2O_3 was most suitable for enhancing the thermal conductivity.

Acknowledgements

The authors wish to express their thanks to Dr. M. Toriyama and Dr. K. Hirao of National Industrial Research Institute of Nagoya (NIRIN) for assisting in the measurement of thermal diffusivity and specific heat data, and to Professor Dr. G. de With, Dr. R.J. Bruls, and Dr. C.-M. Fang of Eindhoven University of Technology for their fruitful discussion.

References

1. Groen, W. A., van Hal, P. F., Kraan, M. J. and de With, G., New high thermal conductivity ceramics. In *Forth Euro Ceramics*, Vol. 3, *Basic Science- Optimization of Properties and Performance by Improved Design and Microstructural Control*, ed. S. Meriani and V. Sergo. Faenza, Italy, 1995, pp. 343–50.
2. Bruls, R. J., Hintzen, H. T. and Metselaar, R., Preparation and characterization of $MgSiN_2$ powders. *J. Mater. Sci.*, 1999, **34**, 4519–4531.
3. Hintzen, H. T., Bruls, R. J. and Metselaar, R., The thermal conductivity of $MgSiN_2$ ceramics. In *Fourth Euro Ceramics*, Vol. 2, *Basic Science—Developments in Processing of Advanced Ceramics—Part II*, ed C. Galassi. Faenza, Italy, 1995, pp. 289–94.
4. Uchida, H., Itatani, K., Aizawa, M., Howell, F. S. and Kishioka, A., Synthesis of magnesium silicon nitride by the nitridation of powders in the magnesium-silicon system. *J. Ceram. Soc. Jpn.*, 1997, **105**, 934–939.
5. Uchida, H., Itatani, K., Aizawa, M., Howell, F. S. and Kishioka, A., Preparation of magnesium silicon nitride powder by the carbothermal reduction technique. *Adv. Powder Technol.*, 1999, **10**, 133–143.
6. Davies, I. J., Uchida, H., Aizawa, M. and Itatani, K., Physical and mechanical properties of sintered magnesium silicon nitride compacts with yttrium oxide addition. *Inorg. Mater.*, 1999, **6**, 40–47.
7. Davies, I. J., Shimazaki, T., Aizawa, M., Suemasu, H., Nozue, A. and Itatani, K., Physical properties of hot-pressed magnesium silicon nitride compacts with yttrium oxide addition. *Inorg. Mater.*, 1999, **6**, 276–284.
8. Slack, G. A., Tanzilli, R. A., Pohl, R. O. and Vandersande, J. W., The intrinsic thermal conductivity of AlN. *J. Phys. Chem. Solids*, 1987, **48**, 641–647.
9. Bruls, R. J., The termal conductivity of magnesium silicon nitride, $MgSiN_2$, ceramics and related materials. Doctoral Thesis, CIP-Data Library Technische Universteit Eindhoven (Eindhoven University of Technology), Eindhoven, The Netherlands, 2000, pp. 163.
10. Ruh, R. and Zangvil, A., Composition and properties of hot-pressed SiC–AlN solid solutions. *J. Am. Ceram. Soc.*, 1982, **65**, 260–265.
11. Niihara, K., Morena, R. and Hasselman, D. P. H., Evaluation of K_{IC} of brittle solids by the indentation method with low crack-to-indent ratios. *J. Mater. Sci. Lett.*, 1982, **1**, 13–16.
12. Liu, D.-M., Chen, C.-J. and Lee, R. R. R., Thermal diffusivity/conductivity in SiAlON ceramics. *J. Appl. Phys.*, 1995, **77**, 494–496.
13. Takahashi, Y., Heat capacity measurements of nuclear materials by laser flash method. *J. Nucl. Mater.*, 1974, **51**, 17–23.
14. Powder Diffraction File Card No. 25-530, JCPDS International Center for Diffraction Data, Newton Square, PA (1975).
15. Powder Diffraction File Card No. 32-1423, JCPDS International Center for Diffraction Data, Newton Square, PA (1982).
16. Powder Diffraction File Card No. 31-1454, JCPDS International Center for Diffraction Data, Newton Square, PA (1981).
17. Powder Diffraction File Card No. 31-1216, JCPDS International Center for Diffraction Data, Newton Square, PA (1981).
18. Powder Diffraction File Card No. 31-506, JCPDS International Center for Diffraction Data, Newton Square, PA (1981).

19. Jack, K. H., Sialon and related nitrogen ceramics. *J. Mater. Sci.*, 1976, **11**, 1135–1158.
20. Cheng, Y.-B. and Thompson, D. P., Aluminum-containing nitrogen melilite phases. *J. Am. Ceram. Soc.*, 1994, **77**, 143–148.
21. Inomata, Y., Yukino, K., Matsunaga, T. and Wada, T., Hot-pressing of Si_3N_4 with magnesium compound additives. *Yogyo-Kyokai-Shi*, 1976, **84**, 534–539.
22. Gaukler, L. J., Hohnke, H. and Tien, T. Y., The system Si_3N_4–SiO_2–Y_2O_3. *J. Am. Ceram. Soc.*, 1980, **63**, 35–37.
23. Bruls, R. J., The termal conductivity of magnesium silicon nitride, $MgSiN_2$, ceramics and related materials. Doctoral Thesis, CIP-Data Library Technische Universteit Eindhoven (Eindhoven University of Technology), Eindhoven, The Netherlands, 2000, pp. 80.